Chapter 3

Materials and Methods

3.1. Plant cultivation

3.1.1. Cultivation of the winter crop, *Brassica napus*, and summer crop *Zea mays*

Seed of the summer crop, *Zea mays*, were planted on 10 November 2009 and the winter crop, *Brassica napus*, were planted on 19 March 2010 respectively, in eighty 16 dm^3 pots (30 cm diameter). The growthmedium used was a mixture of topsoil, river sand and fine vermiculite (2:1:1). To this a six-month slow release fertiliser containing 14N:9P:15K:2MgO (Plantacote® pluss, Aglukon Spezialdünger, GmbH & Co.KG, Heerdter Landstraße 199, D-40549, Düsseldorf, Germany) was homogenically added into each pot. Two treatments (well watered (WW) and drought stressed (DS)) (**Figure 3.1**) were employed using a unique irrigation system (Mills *et al.*, 2005). The pots were placed in open top chambers (OTC's) which allow well controlled treatments whilst ensuring that ecological realism is attained as far as possible. Maize plants were cultivated to full maturity, demonstrating that the treatments were realistic and within the physiological tolerance window of the test plants. Unfortunately, the same could not be done with canola plants since sub-minimum temperatures lead to frost damage just before they reached harvest maturity.

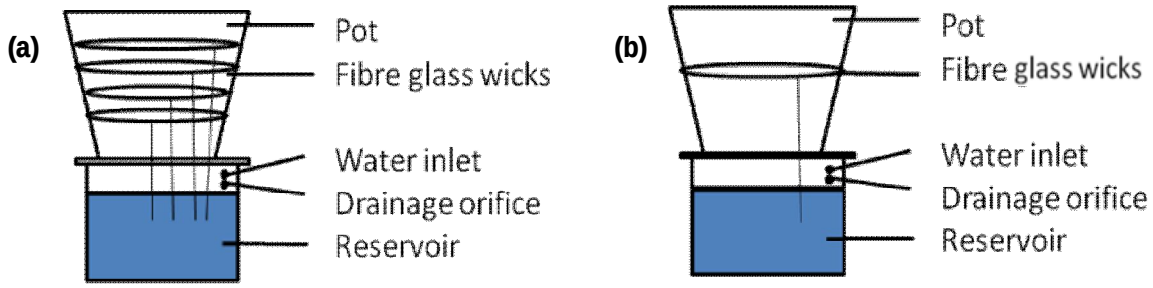

Figure 3.1: Schematic representation of the irrigation system in (a) WW and (b) DS treatments. Potted plants were placed on-top of a reservoir bucket filled with water. In the drought treatment, one fibre glass wick was placed in the soil in the middle of each pot, while for the WW treatments, four fibre glass wicks were placed at four levels in the soil of the pots, hence ensuring uniform irrigation of the plant medium. Glass fliber wicks were let to hang in the water reservoir to conduct water from the pots to the soil by capillary forces (Mills *et al.*, 2005).

3.2. Experimental layout

3.2.1. Open Top Chambers (OTCs) and treatments

OTCs are the internationally accepted method to expose plants to air pollutants and have been widely used in various experiments (Lee *et al.*, 1997; Heyneke *et al.*, 2012b; Bell & Marshall, 2000). This project is a continuation of previous studies on the influence of air pollutants such as O_3 and SO_2 on various crop plants at the OTC-facility, North-West University, Potchefstroom (Heyneke *et al.*, 2012a).

Figure 3.2: Photo of the OTC facility at the Potchefstroom campus, North west University, during the December 2009/ January 2010 maize project, showing six of the twelve OTCs.

Twelve uniquely designed chambers were erected on the Potchefstroom campus of the North West University. These 2.2 m high X 1.7 m wide chambers are fitted with rain caps which are open at the sides, hence the name, “open-top” cambers (**Figure 3.2**). These caps exclude rain from the test

plants, enabling the maintenance and control of a particular water regime. The frames were covered with PVC sheeting that allows more than 90 % PAR transmission (Heyneke *et al.*, 2012a).

In the present study eight OTCs were used: Two chambers were utilised to expose plants to only carbon filtered air (CF), two OTCs for plants exposed to CF air enriched with 50 ppb SO_2, two chambers for plants exposed to CF air enriched with 100 ppb SO_2 and lastly two OTCs with CF air enriched with 200 ppb SO_2. Air is blown into an OTC chamber by means of a blower unit. From where the air folows through a series of three filters to ensure that all impurities (such as air pollutants and dust particles) are removed before entering a chamber. Charcoal filtered (CF) chambers served as control treatments, and open air ('outside') plots were included to assess the chamber effect. The control chambers contained a blend of charcoal and Purafil (Purafil ®, Georgia, USA) in the second series of filters, which removed gaseous pollutants (such as O_3, SO_2 and NO_2) from the air that was not successfully flitered out in the 1st set of filters (Heyneke *et al.*, 2012a). Each OTC has the capacity of housing eight potted plants, thus four of the eight pots inside an OTC represented the DS (~20% of field capacity) and four pots the WW (~80% field capacity) treatments (**Figure 3.3**).

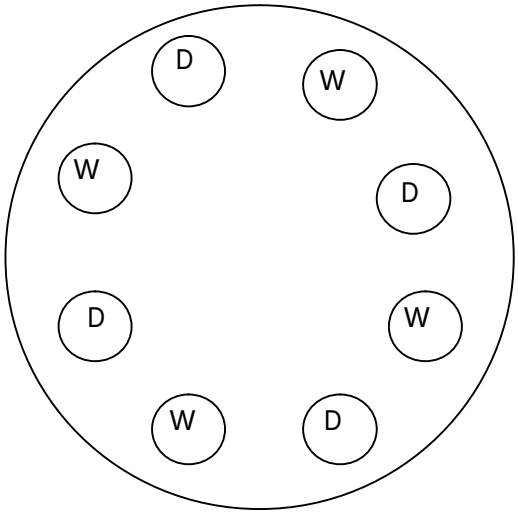

Figure 3.3: A sketch of an OTC with "D" illustrating the position of pots prepared for drought stress treatments, and W pots prepared for the well watered treatments.

A high capacity blower and filter unit with speed control, supply air at an air speed of about 2 $m.s^{-1}$ to a set of two OTCs. A sophisticated SO_2 gas dosage system, employing a series of rotameters feeds SO_2 into the air streams and disperses the gas through perforated toroids (layflat tubing) in the individual chambers (Heyneke *et al.*, 2012a). Every fifteen minutes an air sample within a chamber is analysed in order to monitor the SO_2 levels within each chamber throughout the day. By down loading and analysing the data from this computer driven air sampling system, precise SO_2-administered treatment could be accomplished (**Figure 3.4**). Meteorological data as well as the temperature and relative humidity within the OTCs were monitored and logged over the extent of the project. Typical data collected from these analysers indicate conditions within such an OTC during a summer's day, temperatures increasing with lapse of time, and similarly the high relative humidity which decreases considerably as the day progress, but at the end of the day again increases (**Figure 3.5**).

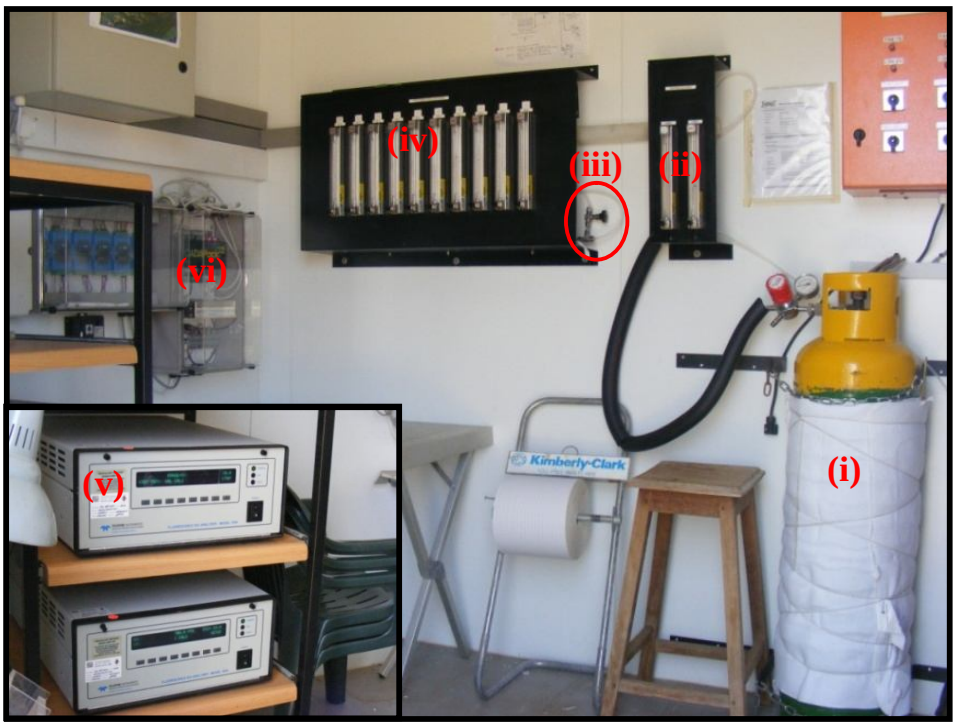

Figure 3.4: The sophisticated SO_2 dosage system comprises, the liquid SO_2 (i) being fed into the first set of rotameters (ii), feeding air and SO_2 into (iii) the gas mixing chamber. The gas mixture (about 20% SO_2) is lead to the second set of rotameters (iv) supplying treatment OTCs with the appropriate dosage of SO_2. Air samples continuously collected from all chambers, are in turn analysed by the SO_2 gas analysers (v). The data is recorded by the logger system (vi).

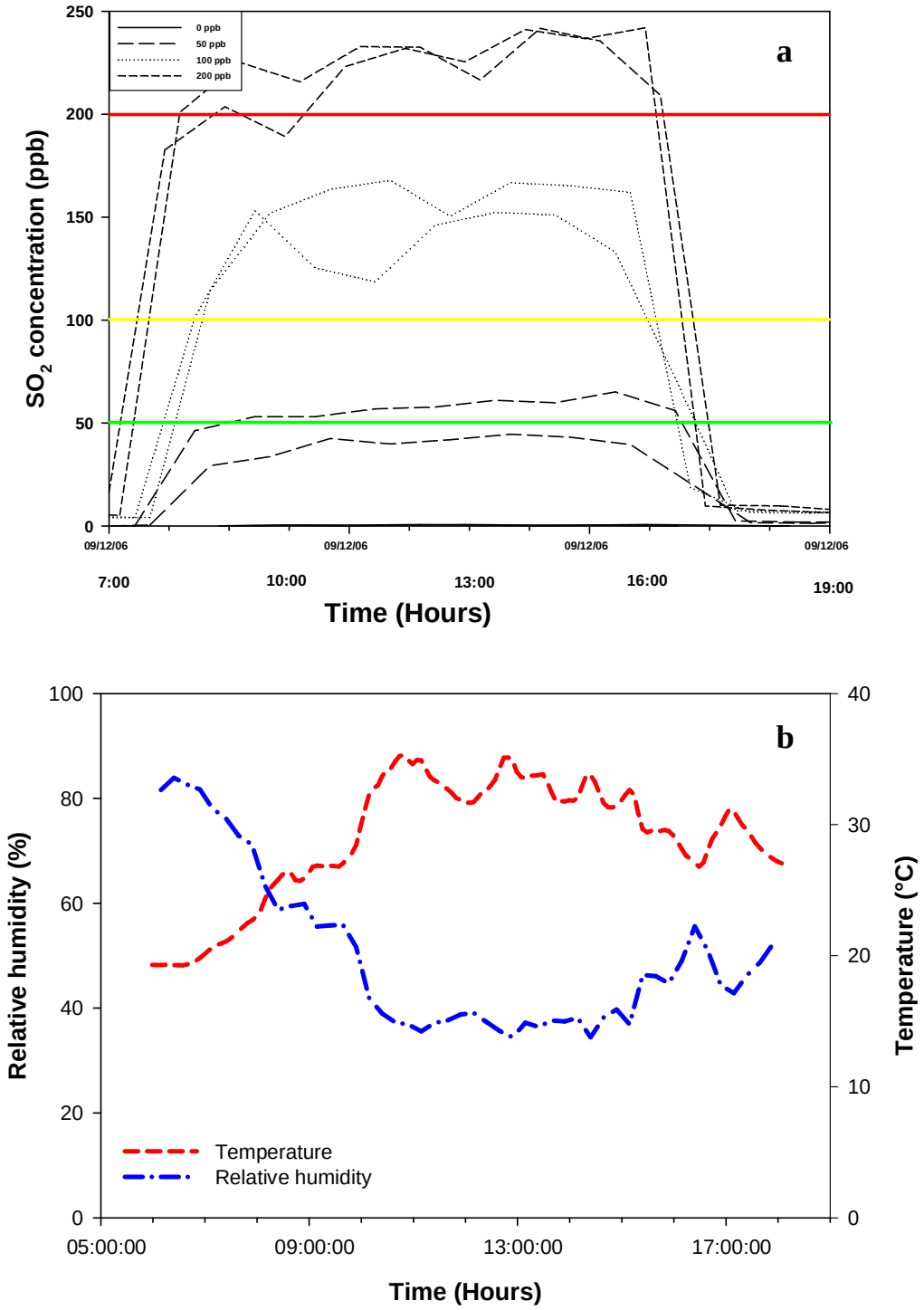

Figure 3.5: An example of a diurnal record of the SO_2 concentrations within the different pairs of OTCs (a); and the typical conditions with regard to temperature and relative humidity inside an OTC during a summer's day, substantiating the fact that the conditions inside the chamber are within an ecologically acceptable range (b).

3.3. Non-destructive plant measurements

The most active photosynthetic tissue in higher plants is the mesophyll of leaves, which renders this organ the primary site of photosynthesis in vascular plants (Stern, 2012). Hence, probing the leaves is the acceptable way to study the effects of various inhibitors of photosynthesis and growth. Non-destructive physiological measurements carried out in this study included the determination of chlorophyll *a* fluorescence induction, photosynthetic gas exchange and determining the chlorophyll content as well as evaluating SO_2 induced leaf damage and growth response. All measurements were carried out in parallel on a two-weekly basis. It is well documented that the function of thylakoid membranes is sensitive to several environmental stresses. PSII including the water oxidising complex (OEC), appears to be particularly sensitive to a number of stress factors (Stirbet & Govindjee, 2011). Since different stresses directly or indirectly affect the function of PSII, chlorophyll *a* fluorescence (though an indirect measure) is an excellent non-invasive tool to study stress responses. Analysis of the OJIP transients by the JIP-test was carried out according to the method described Strasser *et al.* (2004). Photosynthetic gas exchange on the other hand is a direct reflection of physiological performance of the chloroplast and the efficiency of the stomata. Determining the CO_2 response of the test plants enables the quantification of various gas exchange parameters and assessment of the status of the photosynthetic apparatus of the differently treated plants (Lange *et al.,* 1987). For a more detailed discussion on fluorescence measurements see p. 61.

3.3.1. Plant growth and visual symptoms

Throughout the duration of the experiments, the visual damage due to SO_2 was noted. In the maize plants the influence of SO_2 on growth was quantified by measuring the height of the plants, from the base to the flag leaf (**Figure 3.6**) after 12 weeks' fumigation.

3.3.2. Chlorophyll content index

The chlorophyll content index (CCI) was measured using a hand-held Chlorophyll Content Meter (CCM-200, Opti-Sciences, Inc., USA). This data served as a measure of the chlorophyll content in the leaves of test plants at one week, four weeks and seven weeks after onset of fumigation with SO_2.

Figure 3.6: Determining the impact of SO_2 damage on growth by measuring the length of maize plants from the base to the tip of the flag leaf.

3.3.3. Photosynthetic gas exchange

3.3.3.1. Overview of photosynthetic gas exchange kinetics

Studies of CO_2 gas exchange can provide a direct, *in vivo* probe for determining limitations to photosynthetic carbon assimilation, allowing quantitative assessment of the effects of environmental variables on different steps in the diffusion pathway. By simultaneous measurement of CO_2 and water vapour fluxes it is possible to separate stomatal limitations from limitations within the

mesophyll, and to separate effects on the light-limiting and CO_2-limiting phases of photosynthesis (Long & Hällgren, 1993). Understanding what limits photosynthesis in different plants, particularly under sub-optimal climatic conditions in response to atmospheric pollution, has assumed great importance both in agricultural and environmental research. The underlying biochemistry of a leaf can be probed by measuring the response of CO_2 assimilation rate to the intercellular CO_2 partial pressure. This is an instantaneous and non-destructive method which allows simultaneous measurement of the total carbon gain and transpiration by a plant (Lange *et al.*, 1987; Long *et al.*, 1996).

Infrared (IR) gas analysis of CO_2 assimilation is the most widespread contemporary method of determining CO_2 concentrations in the measurement of photosynthetic and respiratory rates of plants (Long & Hällgren, 1993). Using a portable, open-circuit photosynthetic system, air is continuously passed through a leaf chamber to maintain a steady CO_2 concentration in the leaf chamber. The leaf to be analysed was placed in the leaf chamber fitted with an infra-red gas analyser. The main console supplies the chamber with air at a known rate with a known concentration of CO_2 and H_2O. The air is directed over the leaf and the difference between in-coming and out-going air is continuously determined. The CO_2 assimilation rate is expressed in terms of the difference in concentration between C_a and C_i (the driving force for the inward movements of CO_2) and the prevailing stomatal conductance (g_s) (Farquhar & Sharkey, 1982), i.e:

$$A = g_s(Ca - Ci) \text{ (also referred to as the sullpy function).} \quad \text{(i)}$$

The transpiration rate is expressed as:

$$E^* = g_{H_2O}(Wi - Wa), \quad \text{(ii)}$$

where g_{H_2O} represents the stomatal conductance for water vapour, and (Wi – Wa) the difference between ambient water vapour concentration and the water vapour concentration of the sub-stomatal cavity (Long & Hällgren, 1993).

---

* Rate = per time

At any given time, the extent of stomatal opening and its impact on both photosynthesis and water loss will be determined by the sum of all factors influencing stomatal function, and not any one alone. In reality, the stomatal pore itself is not the only barrier to gaseous diffusion between the leaf and its environment. A number of other factors such as unstirred layers on the leaf surface, also called the boundary layer, and the aqueous path between the air space and the chloroplast, offer resistance to the uptake of CO_2 into the leaf (Saupe, 2009). Since CO_2 intake and H_2O release both occur through the stomata, high rates of CO_2 uptake are expected to coincide with high rates of transpiration. A high stomatal conductance would thus promote high rates of CO_2 uptake and H_2O loss (Read *et al.,* 2009). A net influx of CO_2 into the leaf occurs in photosynthesis because of a diffusion gradient. Before CO_2 can enter the stomatal apature it first has to diffuse through the boundry layer on the leaf surface.

In the Parkinson-type leaf chamber (used in most portable systems and also in the present study) the boundary layer resistance is minimised and kept constant by removing this layer. This is made possible a fan inside the leaf chamber (LC) drives a high turbulent movement over the surface of the leaf. If only diffusion is taken into consideration, the intercellular CO_2 concentration (C_i) can be determined by:

$$C_i = C_a - A/g_i \qquad \text{(iii)}$$

where g_i represents the total conductance, i.e. boundry layer as well as stomatal conductance, and C_a is the atmospheric CO_2 concentration.

A CO_2-response curve, also called an A:Ci curve, can be generated (**Figure 3.8**) by plotting the photosynthetic assimilation rate (A) against the intercellular CO_2 concentration (Ci) inside the substomatal space calculated from (i), when the leaf inside the PCL is exposed to a known CO_2 concentration (C_a). By measuring the photosynthetic assimilation rate at increasing CO_2 concentrations an artificial situation can be created where no stomatal limitation exists (Ci = Ca). The photosynthetic CO_2 assimilation rate under such conditions is then used as reference point to calculate the percentage stomatal limitation (Farquhar & Sharkey, 1982; Von Caemmerer & Farquhar, 1981; Lange *et al.,* 1987).

Changes in gas exchange parameters are excellent indicators of the limitations on the photosynthetic apparatus due to environmental stressors. These gas exchange parameters can be deduced from the CO_2-response curve and the values used as a quantitative measure of the extent to which the environmental stressors are responsible for limiting in photosynthesis. It is possible to separate limitations in the mesophyll from stomatal limitations by employing simultaneous measurements of CO_2 and water vapour fluxes (Farquhar & Sharkey, 1982; Long & Hällgren, 1993). Except for the mentioned parameters which can be deduced from the A:Ci curve, functions can be derived from (i) the initial slope of the rising part of the function, called the demand function ($A = CE(Ci - \Gamma)$), and (ii) from the intersecting function at Ci_{370}, namely the supply function ($A = g_s(Ca - Ci)$). The demand function expresses the rate of CO_2 assimilation in terms of the carboxylation efficiency and the capacity of the system to assimilate CO_2 (Farquhar & Sharkey, 1982). The initial slope of the CO_2-response curve (CE) can be correlated to *in vitro* measurement of Rubisco activity in C_3 plants (Von Caemerer & Farquhar, 1981; Bolhàr-Nordekampf & Öquist, 1993) and in C_4 plants it is an estimation of PEPcase activity. The maximal CO_2 assimilation rate at saturating Ci (J_{max}) can be regarded as a reliable indicator of the maximum electron transport rate and as the RuBP regeneration capacity of the leaf which also depends on the capacity for electron transport (Von Caemerer & Farquhar, 1981; Farquhar & Sharkey, 1982). Γ represents the CO_2 compensation concentration which can be defined as the CO_2 concentration at which net efflux of CO_2 from the plant is zero, in other words the point at which CO_2 assimilated during photosynthesis is equal to the rate at which CO_2 is produced during respiration, mainly during the process of photorespiration. At the intersection point of the demand- and supply functions we find the assimilation rate at C_a (370 $\mu mol.mol^{-1}$ CO_2), i.e. A_{370}. This point is representative of the actual assimilation rate at ambient conditions and is also known as the operational point (Lange *et al.*, 1987).

The following equation is used to determine the degree of stomatal limitation occurring in a photosynthesising plant (ℓ) and expressed as a percentage:

$$\% \ \ell = [(A_0 - A_{370}) / A_0] \times 100 \qquad \text{(iv)}$$

where A_{370} represents the CO_2 assimilation rate at ambient CO_2 concentration (Ca = 370 $\mu mol.mol^{-1}$) and A_0 the assimilation rate where no stomatal limitation is present ($Ci \geq 370$ $\mu mol.mol^{-1}$) (Farquhar & Sharkey, 1982).

The water use efficiency (WUE) can be defined as the ratio of CO_2 assimilation into the photosynthetic biochemistry (A) to water lost during transpiration by the stomata (E) (Griffiths, 1993; Bacon, 2004). This term describes a plant's photosynthetic production rate relative to the rate at which it transpires water to the atmosphere. It is a measure of plant performance that has long been of interest to agronomists, foresters and ecologists (Bacon, 2004). In cropping systems, improving water-use efficiency presents a means of increasing crop production in the face of finite water supplies (Richards *et al*., 2002). Water use efficiency (WUE) was determined with the following formula:

$$WUE = A_{370} / E_{370} \qquad (v)$$

where A_{370} represents the CO_2-assimilation rate at ambient CO_2 concentrations, and E_{370} the transpiration rate at ambient CO_2 concentrations. WUE is expressed in mmoles CO_2 assimilated per mole H_2O transpired.

3.3.3.2. Photosynthetic gas exchange measurements on *Brassica napus* and *Zea mays*

Changes in CO_2 gas exchange was measured using a portable infra red gas analyser with automatic leaf chamber (CIRAS 2, PP Systems, UK). Measurements were conducted every two weeks (see detailed procedure on p. 56), using a standard broad leaf photosynthetic chamber (PLC) placed over the measured leaf, exposing a 2.5 cm^2 section leaf area to differing CO_2 concentrations (**Figure 3.7**).

Figure 3.7 (right): Measuring Photosynthetic gas exchange with an infrared gasanalyser (IRGA) on a mature maize leaf during the December 2009/ January 2010 experiment.

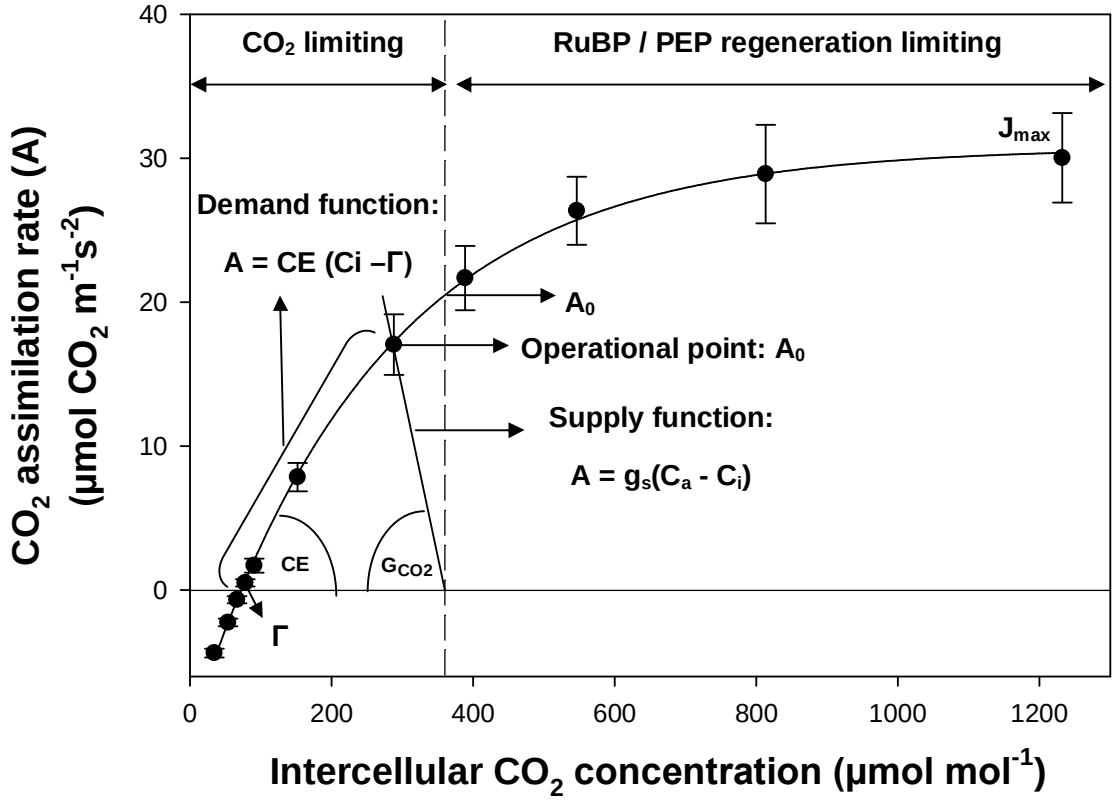

Figure 3.8: A typical CO_2 response curve with the CO_2 assimilation rate (A) vs. intercellular CO_2 concentration (Ci). The assimilation rate under atmospheric conditions is denoted as A_{370}, i.e. the point of simultaneous solution of the demand and supply functions. The carboxylation efficiency (CE) is represented by the initial slope of the demand function, the CO_2 compensation concentration (Γ) is the mole fraction of CO_2 at the point on the x-axis (intercellular CO_2 level) where the net usage of CO_2 equals zero; the maximum point of CO_2 assimilation on the A:Ci curve (J_{max}) represents the rate of CO_2 assimilation at saturated levels of CO_2 (the RuBP regeneration capacity) and A_0 is the rate of assimilation at the point where stomatal limitation is artificially eliminated by raising the internal CO_2 concentration (Ci) to equal the atmospheric CO_2 concentration (interpolation of the value of A from the response curve at Ci=370 µmol.mol^{-1}) (Lange *et al.*, 1987). With the data collected by an IRGA (dots on the graph) the A:Ci plot was constructed.

3.3.4. Fast phase chlorophyll *a* fluorescence kinetics

3.2.3.1. Overview of direct chlorophyll *a* fluorescence

Before the concept of chlorophyll *a* fluorescence can be fully grasped, an understanding of the working of electron transport and energy transfer within the thylakoid membrane and PSII is necessary. Chlorophyll *a* fluorescence is linked with numerous processes taking place during the energy conversion of light into a stable chemical form (Stirbet & Govindjee, 2011). The concept of electron flow within the electron transport chain (ETC) is made easy by an illustration of the photosynthetic electron transfer from water to $NADP^+$, which can be fit into the framework of a Z-scheme (**Figure 3.9**) (Govindjee & Veit, 2010).

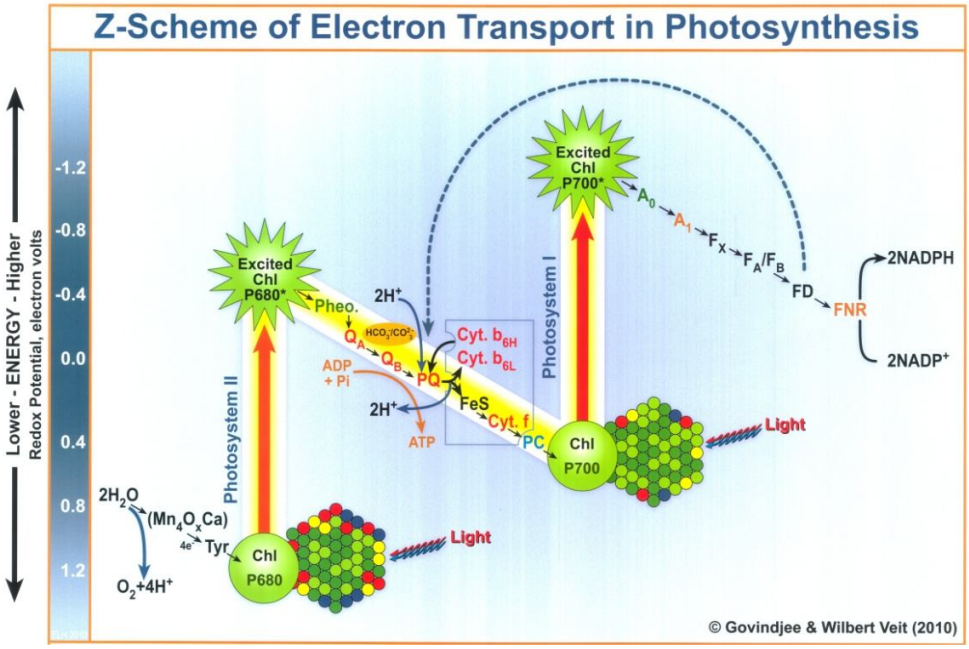

Figure 3.9: The Z-Scheme of electron transport in photosynthesis (Govindjee & Veit, 2010).

The diagram illustrating the process of energy transfer within the thylakoid membrane shows how light energy is passed from one acceptor to the next. The antennae molecules of PSII (P680) is excited by light energy, the photons is then transferred to pheophytin, the plastoquinone pool and eventually plastocyanin. From here (together with more excitation energy) energy are transferred from PSI (P700) to the electron acceptor ferredoxin oxidoreductase to eventually yield and energy rich molecule NADPH. In addition several ATP molecules are produced during this process, which

drive the PCR cycle. During photosynthesis a portion of the light energy, absorbed by the chlorophyll molecules is always lost as heat or by re-emission as chlorophyll fluorescence (Papageorgiou & Govindjee, 2004; Bolhàr-Nordenkampf & Öquist, 1993). Since these decay processes of excited chlorophyll are competitive, changes in the photosynthetic rate and/or in dissipative heat emission will cause complementary changes in the intensity of the emitted fluorescence. Chlorophyll fluorescence informs on the identity of the various pigments and pigment complexes, their organization, excitation energy transfer among them, and on the various electron-transfer reactions, specifically of PSII (Govindjee, 2004). This measure is thus directly related to the activity of chlorophyll in the photosynthetic reaction centers and is a useful, direct, and integrated measure of photosynthetic function and plant stress (Cavender-Bares & Bazzaz, 2004). It provides a valuable tool for plant ecologists for use at the leaf level to the ecosystem level (Genty *et al.*, 1989; Oukarroum *et al.*, 2007).

Presently, chlorophyll *a* fluorescence is used as a sensitive, *in vivo* probe of photosynthetic function, both in the field and in the laboratory (Bolhàr-Nordenkampf & Öquist, 1993; Stirbet & Govindjee, 2011). After illuminating a dark adapted leaf with a continuous light source, the excited chlorophyll molecules are stable for less than 10^{-8}s. During this short period a charge separation within the reaction centre takes place, comprising the primary photochemical step of photosynthesis and is indicated as an immediate rise in the fluorescence to a so-called minimal level F_0. At this point all the RCs are open for primary photochemistry, i.e. all electron carriers are oxidised. The F_0 signal provides a valuable reference for all other fluorescence parameters of the induction curve. If the charge separation (P_{680}^{+} $Pheo^{-}$) does not take place, the absorbed light energy is dissipated as heat and/or fluorescence when the excited electron of the molecule returns to ground level. If all PSII RCs are closed, 95% - 97% of the absorbed energy may be deactivated via heat and 2.5 – 5.0% via fluorescence (Bolhàr-Nordenkampf & Öquist, 1993). Generally, fluorescence yield is highest when photochemistry and heat dissipation are lowest. Therefore, changes in the fluorescence yield reflect changes in photochemical efficiency and heat dissipation (Fluoromatics software, 2010).

The fast phase of the fluorescence induction curve when plotted on a logarithmic time scale (**Figure 3.10**) shows different steps during the transient, namely the steps OJIP when plotted on a logarithmic scale (Strasser & Strasser, 1995) and in some instances a K-step is also visible at

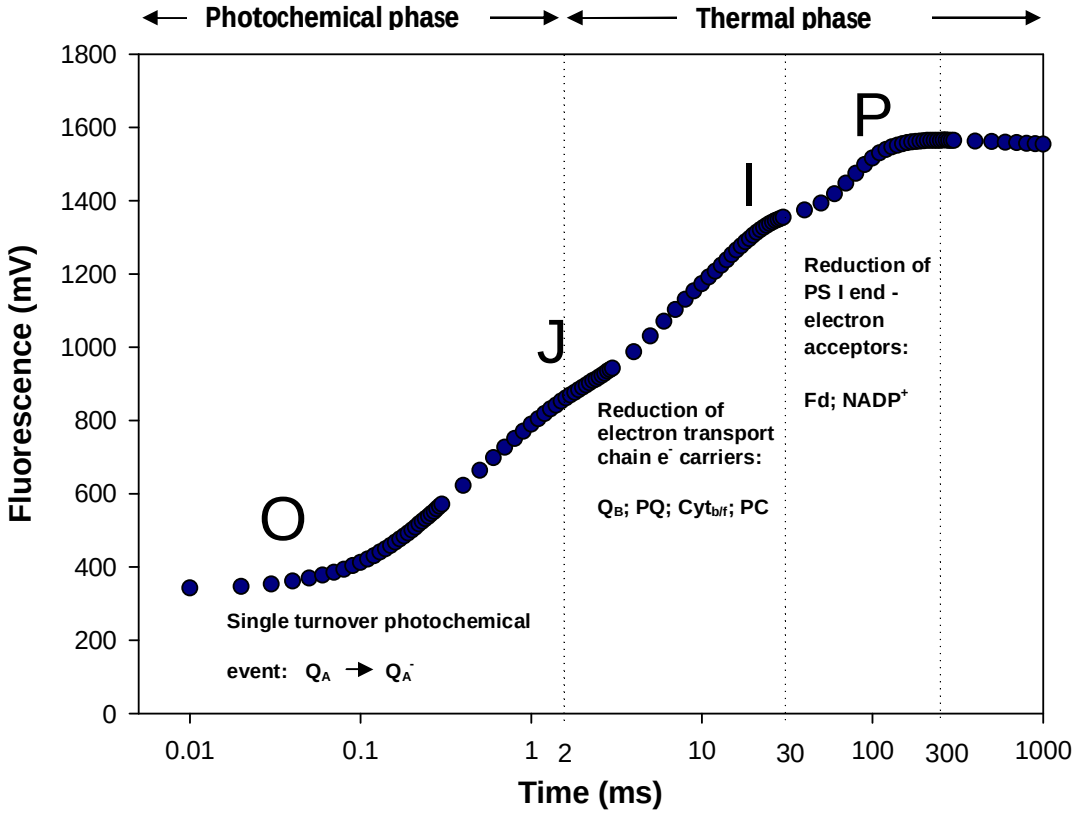

Figure 3.10: Typical fast phase chlorophyll *a* polyphasic fluorescence rise OJIP. The average transient is plotted on a logarithmic time scale from 10 µs to 1 s. The intensity shows characteristic changes called the fluorescence induction, fluorescence transient, or simply the Kautsky effect, within a single second. The energy fluxes through PSII and other parameters of the fast fluorescence rise include a minimum fluorescence intensity level "O" (for "origin", or initial fluorescence at approximately 20 µs) considered as F_0, the maximum fluorescence intensity (F_P) at approximately 300 ms to one second; fluorescence intensity at 300 µs (F300 µs) (required for the calculation of the initial slope (M_0) of the relative variable fluorescence (V) rise); fluorescence intensity at 2 ms (the J step) denoted as F_J and another intermediary step, F_I, is noticeable at 30 ms (Papageorgiou & Govindjee, 2011; Stirbet & Govindjee, 2011; Strasser *et al.*, 2004).

approximately 300 µs (Stirbet & Govindjee, 2011). The fluorescence rise from O to P occurs during the first second of illumination and is called the 'fast phase', which displays characteristic changes in intensity accompanying the induction of photosynthetic activity (Fluoromatics software, 2010). The 'slow phase' follows after P and may take several minutes before the terminal phase, T, is reached. The fast phase is related to primary processes of PSII, whereas the slow phase is mainly related to interactions between processes in the thylakoid membranes and metabolic processes in the stroma, primarily carbon metabolism (Bolhàr-Nordenkampf & Öquist, 1993). The fast rise reflects a gradual increase in the yield of chlorophyll *a* fluorescence, as the rate of photochemistry concurrently declines. The reason for this decline is that Q_A, the primary quinone acceptor of PSII, becomes increasingly reduced as the open RCs close. At step I of the transient the electrons start to become transferred via Q_B to the plastoquinone pool. If the actinic light is strong enough, then all active RCs become closed at P and the maximum level of fluorescence (F_M) is attained, with no photochemistry taking place (Thus $F_M = F_P$) (Bolhàr-Nordenkampf & Öquist, 1993; Stirbet & Govindjee, 2011).

The redox state of Q_A is determined by its photochemical reduction due to PSII activity and its re-oxidation by the electron transport driven by PSI activity. When Q_A in a RC is reduced (Q_A^-) the RC is closed and the chlorophyll fluorescence of the antenna is high, whereas when the Q_A is in the oxidized state, the RC is open and the fluorescence of the antenna is quenched. As Q_A becomes partially oxidised through electron transfer to PSI via the cytochrome f/b_6 complex and plastocyanin, the fluorescence decreases (Bolhàr-Nordenkampf & Öquist, 1993)

Early researchers employed fluorometry in order to elucidate the measure of photosynthetic activity of the photosystem, of which chlorophyll *a* fluorescence values is an inverse measure. Chlorophyll *a* fluorescence emission is influenced by (Papageorgiou & Govindjee, 2011):

1. Redox active chlorophyll *a* molecules in the RC of PSII (photochemical quenching)
2. An electrochemical imbalance across the thylakoid membrane (high energy quenching), and
3. The size of the peripheral antennae of weakly fluorescent PSII in response to changes in the ambient light (state transitions)

The derivation of the links between the biophysics of the photosynthetic apparatus and the fluorescence signals and their analytical formulation is based on the 'Theory of Energy Fluxes in Biomembranes' (Strasser *et al.*, 2004) and on the basic concept that the fluorescence yield of PSII is determined by the state – open or closed – of the reaction center. The approach taken for the analysis of the chlorophyll fluorescence transients in the present study is also adopted by the majority of researchers, known as the dogma that the state of PSII RCs is defined only by the redox state of the PSII primary quinone acceptor Q_A.

3.3.4.2. Analysis of the fast phase chlorophyll fluorescence transient O-J-I-P by the JIP test

Analysis by the JIP-test of the O-J-I-P fluorescence transients provides a wealth of information, even though the transients are obtained from a leaf at a **dark adapted** state. This analysis of strong actinic light-induced fluorescence rise kinetics (O-J-I-P) by the JIP-test can be applied at any physiological state and for the study of any state transition including the analytical derivation of formulae for the translation of selected data stored in the OJIP transient to structural and functional parameters quantifying PSII behaviour. The calculated parameters are: the so-called 'specific' (per reaction centre, RC) and 'phenomenological' (per excited cross section, CS, of a photosynthetic sample) energy fluxes of absorption, trapping and electron transport; the quantum yields of primary photochemistry and of electron transport, as well as the efficiency by which a trapped exciton moves an electron into the electron transport chain further than Q_A; the density of Q_A^- reducing RCs which, by comparison of samples under different conditions, leads to the calculation of the difference in the fraction of non-Q_A reducing RCs (heat sinks or 'silent' centers); the so-called 'performance indexes' and 'driving forces'; the turnover number expressing the number of Q_A reduction events untill all Q_A molecules are reduced (Strasser *et al.*, 2004).

The maximum specific trapping flux at time = 0 is expressed as the ratio TR_0/RC, which is also a key expression of the JIP-test. At any time the specific trapping flux TR_t/RC expresses the rate per RC by which excitons are trapped by RCs resulting in the reduction of Q_A to Q_A^- i.e., to the increase of the fraction of closed RCs; hence TR_t/RC (in arbitrary units) is equal to dV/dt. In an experiment where samples are treated with DCMU, consequently blocking the process of re-oxidation of Q_A^-, the reduction of Q_A through a single turn-over reflect the primary photochemical reactions which are calculated using the initial slope of the fluorescence rise:

$$(dV/dt)_{0,\,DCMU} = M_{0,\,DCMU}$$

The initial slope ($\Delta V/\Delta t$) which is now denoted as $M_{0,}$ expresses the net rate of RC closure where trapping flux increases the number of RCs and electron transport flux decreases it. By thus denoting ET_0/RC the specific flux at time zero of electron transport beyond Q_A^- we get:

$$M_0 = TR_0/RC - ET_0/RC$$

Strasser & Strasser (1995) discovered that by multiplying M_0 by $1/V_J$ (V_J is the relative change in fluorescence at F_J, calculated by $(F_J - F_0)/(F_M - F_0)$) one can retrieve data which simulate the DCMU effect, in other words:

$$TR_0/RC = M_{0,\,DCMU} = M_0/V_J$$

The latter finding is the key element of the JIP test.

The 'performance index' ($PI_{ABS.total}$) provides a measure of the potential of the whole photosynthetic electron transport chain for light energy conversion into redox energy. This expression is the product of terms expressing potentails for photosynthetic performance at each energy bifurcation from excitation to the reduction of PSI and end acceptors (Luo *et al.*, In press), namely the fluxes of absorption (ABS), trapping (TR), electron transport (ET) and reduction of end electron acceptors (RE). The initial stage of photosynthetic activity of a RC complex is regulated by three functional steps namely absorption of light energy (ABS), trapping of excitation energy (TR) the conversion of excitation energy to electron transport (ET) and the reduction of end electron acceptors (RE). The photosynthetic performance index ($PI_{ABS.tot}$), is based on the fast phase chlorophyll fluorescence rise and is a multi-parametric function taking into account these four partial processes of primary photochemistry. It is expressed by the following equation (Strasser, 2000; Smit *et al.*, 2009; Yusuf *et al.*, 2010):

$$PI_{ABS.total} = \frac{\gamma_{RC}}{1-\gamma_{RC}} \cdot \frac{\varphi_{Po}}{1-\varphi_{Po}} \cdot \frac{\psi_{Eo}}{1-\psi_{Eo}} \cdot \frac{\delta_{Ro}}{1-\delta_{Ro}}$$

**Table 3.1. Summary of the JIP-test formulae using data extracted from the fast fluorescence transient O-J-I-P. (Modified from Strasser *et al.*, 2000). ***see footnote p. 68

Extracted and Technical Fluorescence Parameters	
F_0	= $F_{50\mu s}$, fluorescence intensity at 50µs
$F_{100\mu s}$	= fluorescence intensity at 100µs
$F_{300\mu s}$	= fluorescence intensity at 300µs
F_J	= fluorescence intensity at the J-step (at 2ms)
F_I	= fluorescence intensity at the I-step (at 30ms)
F_M	= maximal fluorescence intensity
t_{FM}	= time to reach F_M, in ms
V_J	= relative variable fluorescence at the J-step = $(F_{2m}s - F_0)/(F_M - F_0)$
$(dV/dt)_0 = M_0$	= fractional rate of PSII reaction centre closure = $4.(F_{300} - F_0)/(F_M - F_0)$
Quantum Efficiencies or Flux Ratios or Yields	
$\varphi_{Po} = TR_0/ABS$	= $[1 - (F_0/F_M)] = F_V/F_M$
$\varphi_{Eo} = ET_0/ABS$	= $[1 - (F_0/F_M)]. \Psi_0$
$\varphi_{Ro} = RE/ABS$	= $(1\text{-}V_I)/(1\text{-}V_J)$
$\Psi_0 = ET_0/TR_0$	= $(1\text{-}V_J)$
Specific Fluxes or Specific Activities	
ABS/RC	= $M_0 . (1/V_J . (1/\varphi_{Po})$
TR_0/RS	= $M_0 . (1/V_J)$
ET_0/RS	= $M_0 . (1/V_J) . \Psi_0$
DI_0/RS	= $(ABS/CS) - (TR_0/RC)$
Phenomenological Fluxes or Phenomenological Activities	
ABS/CS	= ABS/CS_{Chl}/CS or $ABS/CS_0 = F_0$ or $ABS/CS_M = F_M$
TR_0/CS	= $\varphi_{Po} . (ABS/CS)$
ET_0/CS	= $\varphi_{Po} . \Psi_0 . . (ABS/CS)$
DI_0/CS	= (ABS/CS)
Density of Reaction Centres	
RC/CS	= $\varphi_{Po} . (V_J/M_0 . ABS/CS$
Performance Indices	
PI_{ABS}	= $(RC/ABS) . [\varphi_{Po}/(1- \varphi_{Po})] . [\Psi_0/(1- \Psi_0)]$

PI_{TOT}	$= (RC/ABS) . [\varphi_{Po} / (1- \varphi_{Po})] . [\Psi_0 / (1- \Psi_0)] . [\varphi_{Ro}/(1- \varphi_{Ro})]$
Driving Force	
DF_{ABS}	$= \log [PI_{ABS}]$
DF_{TOT}	$= \log [PI_{TOT}]$

*Subscript "o" indicates that the parameter refers to the onset of illumination, when all RCs are assumed to be open

According to Strasser *et al.* (2004) and Yusuf *et al.* (2010) the different parameters are:

γ = $\mathbf{Chl_{RC} / Chl_{total} = Chl_{RC} / (Chl_{RC} + Chl_{antenna})}$. This parameter represents the ratio of reaction center chlorophylls and the total chlorophyll of PSII. The expression $\gamma_{RC} / (1 - \gamma_{RC})$ is proportional to the parameters estimated by JIP-test as equal to the ratio of reaction centers and the absorbance (RC/ABS).

$\mathbf{\varphi_{Po}}$ = $\mathbf{1- (F/F_M) = (FV/FM) = (TR/ABS)}$. This parameter, known as the maximum quantum yield of primary photochemistry corresponds to the efficiency by which an absorbed photon will be trapped by PSII reaction centers.

$\mathbf{\Psi_{Eo}}$ = $\mathbf{1 – Vj = [1- (F_j-F_o/F_M-F_o)] = ET_o/TR_o}$. This is the fraction of electrons transported beyond Q_A^- per exciton trapped by the reaction centers (RC) of PSII. It is the probability that the energy of a trapped exciton is used for electron transport.

$\mathbf{\delta_{Ro}}$ = $\mathbf{(1 – V_i)/(1 - V_j) = [1- (F_i – F_o)/(F_M – F_o)] / [1- (F_j – F_o)/(F_M – F_o)] = RE_o/ET_o}$. This represents the probability to reduce an end electron acceptor using V_j and V_i.

3.3.4.3. Chlorophyll fluorescence induction measurements on *Zea mays* and *Brassica napus*

Chlorophyll *a* fluorescence measurements were conducted weekly with a Handy PEA fluorimeter (Plant Efficiency Analyzer, Hansatech Instruments Ltd., UK) on physiologically mature leaves of both *Zea mays* and *Brassica napus* experimental plants which were dark adapted for one hour or more. Measurements were conducted on four test plants per treatment. Measurements were carried out between 20:00 and 22:00 in darkness to facilitate measuring many samples quickly.

Induction curves were further analysed by calculating the difference in variable fluorescence between the treatment and the control ($\Delta V_t = V_{treatment} - V_{control}$), i.e. subtracting fluorescence values of the controls from the treatments of transients normalised between F_o (0.001 ms) and F_P (300 ms to one second) ($\Delta V_{OP} = V_{OP,treatment} - V_{OP,control}$). In doing so hidden bands can be elucidated in a graph known as the ΔV_{OJ} fluorescence transient.

The JIP-test represents a translation of the original recorded data to biophysical parameters that quantify the step-wise energy flow through PSII (Strauss, 2008). Selected phenomenological and specific parameters as well as the performance index and its parameters ($PI_{ABS.total}$) (already described in previous pages), were presented on a spider plot. The parameters which all refer to time zero (onset of fluorescence induction) are: (i) the specific energy fluxes (per reaction centre) for absorption (ABS/RC), trapping (TR_0/RC) and electron transport (ET_0/RC); (ii) the flux ratios or yields, i.e. the maximum quantum yield of primary photochemistry ($\varphi_{Po} = TR_0/ABS = F_V/F_M$), the efficiency ($\psi_0 = ET_0/TR_0$) with which a trapped exciton can move an electron into the electron transport chain further than Q_A^-, the quantum yield of electron transport ($\varphi_{Eo} = ET_0/ABS = \varphi_{Eo} \cdot \psi_0$); (iii) the phenomenological energy fluxes (per excited cross section, CS) for absorption (ABS/CS), trapping (TR_0/CS) and electron transport (ET_0/CS) (Krüger *et al.*, 1997). The fraction of active PSII reaction centres per excited cross section (RC/CS) is also calculated. Each of the parameters were plotted on spider plots for the 50, 100 and 200 ppb treatments and compared against the carbon filtered control treatment for both WW and DS treatments.

3.4. Destructive measurements

3.4.1. Water potential and relative water content

In general, biomass production is directly proportional to the supply and use of water. Therefore measurement of plant water status is an important part of understanding biomass and yield responses under irrigation. Ideally, both water content and water potential should be measured in experiments, though the nature of the experiment may dictate that only one of the two could be measured (Beadle *et al.*, 1993).

Water potential (ψ) according to Beadle *et al.* (1993) can be defined as the potential energy (joules) per unit mass of water (m^3) with reference to pure water which has the highest potential, namely zero. All other aquous suspensions and solutions in most biological systems thus has less potential energy than pure water which result in negative potential values for the relevant sample. The method used in this project to determine the water potential in test plants is called the pressure chamber technique. Hence the fact that this method is a simple, cheap and rugged it is ideally suited for field studies. The pressure applied to the leaf inside the pressure chamber (**Figure 3.11**) to return the water interface to where it was before detachment, is equal and opposite to the tension in the xylem of the intact plant. Because the osmotic potential of xylem sap is usually greater than -0.02 MPa, the hydrostatic pressure in the xylem is equal to the water potential (Beadle *et al.*, 1993). For a plant cell ψ, which is measured in MPa, may be expressed as the sum of three components:

$$\Psi = P + \pi + \tau$$

where P is the hydrostatic pressure (turgor pressure) arising from pressure exerted on the cells by their walls; π is the osmotic potential arising from the presence of dissolved solutes in the cell; and a third component, τ, which is the matrix potential. This last parameter can also drive osmosis, but compared to the values of P and π, its contribution to the symplast is negligible (Koide *et al.*, 1989; Beadle *et al.*, 1993).

Relative water content (RWC) is the appropriate measure of plant water status in terms of the physiological consequence of cellular water deficit (Anon, 2012). Leaf water status is intimately related to several leaf physiological variables, such as leaf turgor, growth, stomatal conductance, transpiration, photosynthesis and respiration (Kramer & Boyer, 1995). Leaf water content is a useful

indicator of plant water balance, since it expresses the relative amount of water present on the plant tissues (Yamasaki & Dillenburg, 1999). The relative water content in plant material is based on the measurement of the fresh weight (W_f) at time of sample, the dry weight (W_d) and turgid weight (W_t) which is obtained by floating the leaf discs on water at the light compensation point until constant weight is reached (Beadle *et al.*, 1993) (**Figure 3.12**):

$$\text{Relative water content (RWC)} = \frac{Wf - Wd}{Wt - Wd} \text{ X } 100\ \%$$

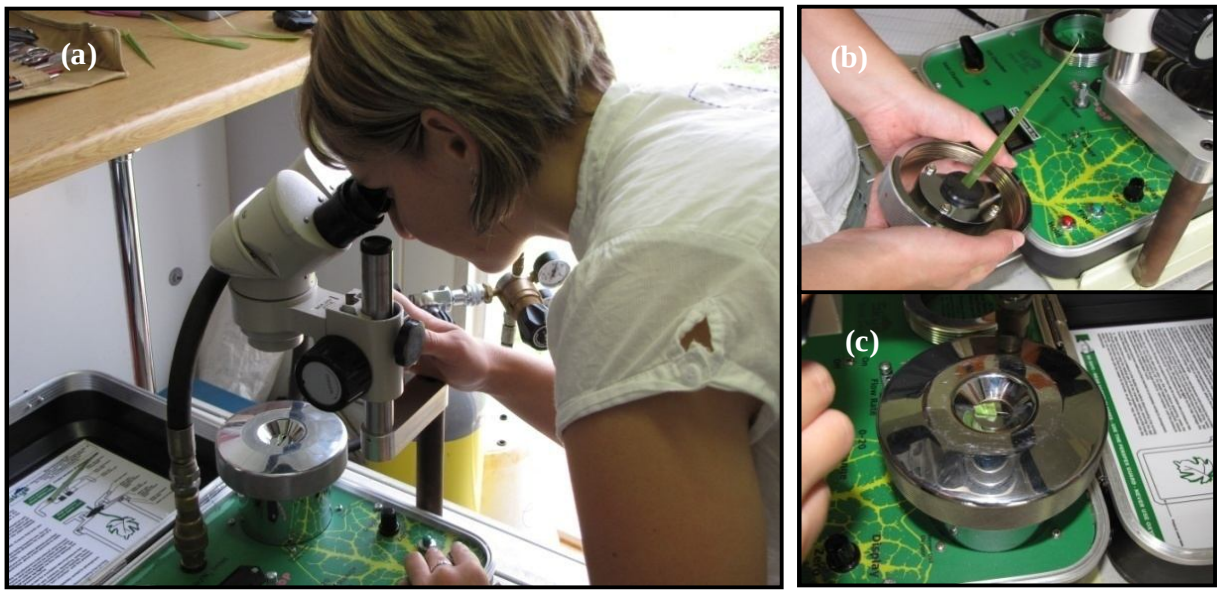

Figure 3.11: Measuring leaf water potential using a Scholander pressure chamber (a). A segment of leaf is cut and placed in the chamber with the cut end projecting throught the hole in a rubber bung (b & c).

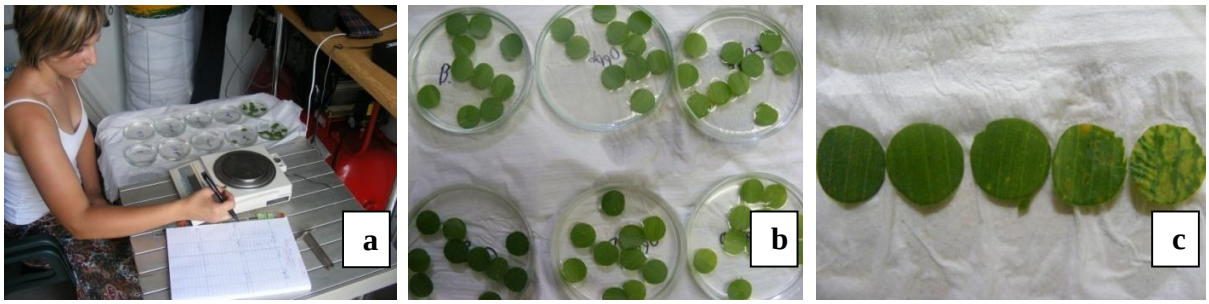

Figure 3.12: Determining relative water content in *Zea mays*, determining (a) Wf and (b & c) Wt.

3.4.2. Environmental Scanning Electron Microscopy (ESEM)

Leaf samples were prepared according to the standard laboratory technique. The harvested leaf material from all treatments (which were stored in 70% ethanol) were dehydrated successively in 90% ethanol and twice in 100% ethanol for ten minutes. This was followed by critical point drying. The critical point drying technique requires that the 100% ethanol within the samples is replaced with liquid CO_2. The CO_2 is then released by heating the chamber of the critical point dryer to the critical point for CO_2 (31° C), which turns the CO_2 into vapor with no surface tension. After critical point drying, the material was mounted on specimen stubs and sputter-coated with gold/palladium. In all cases the epidermal anatomy of the specimens were examined and micrographs were taken with a FEI Quanta 200 environmental scanning electron microscope (ESEM). The photos presented in this thesis were chosen as representitive of each treatment, namely CFWW, 50WW, 100WW, 200WW, CFDS, 50DS, 100DS, 200DS. The relative % stomatal aperture of each treatment was determined by enlarging the photos of the stomata of each respective treatment. The area on the photo representing the stomatal apperture was removed and weighed. Percentage stomatal apperture relative to the control was calculated.

3.4.3. Biomass and Yield

After harvest maturation was achieved (≈ 12 weeks after emergence) the cobs of maize plants were harvested and the cob mass at 12.5 % moisture content was determined usin the following formula:

Cob mass @ 12,5 % moisture content = [a] x [(100-b)/87,5],

where **a** represents the cob mass (fresh weight), **b** represents the % moisture of grain kernels (**Figure 3.13**).

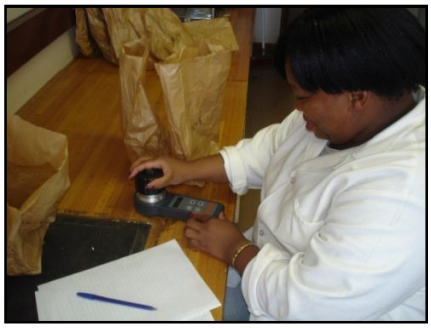

Figure 3.13 (opposite): Determining the percentage moisture content of maize kernels using a hand held % moisture content analyser (provided by the ARC, NW province).

The shoot biomass of canola plants were harvested and determined after 7 weeks' exposure to SO_2 fumigation.

3.4.4. Biochemical analysis

POD enzyme activity, H_2O_2 content and protein concentration of all treatments in maize plants (CFWW, 50WW, 100WW, 200WW, CFDS, 50DS, 100DS and 200DS) were determined after three sampling times, namely at 3 weeks (16 December 2009), 6 weeks (4 January 2010) and 9 weeks' (30 January 2010) of fumigation with SO_2, respectively. The Rubisco activity of canola plants was determined after 6 weeks fumigation with SO_2.

3.4.4.1. Leaf sampling

In maize and canola plants, whole leaves were collected in parallel with fluorescence and photosynthetic gas exchange measurements. Leaf samples were placed in alluminium foil bags and immediately placed in liquid nitrogen to ensure the preservation of enzyme activity at the moment of sampling. Samples were stored at - 80°C. The peroxidase activity (POD) for each respective treatment was determined, as well as the H_2O_2 content. Additional leaf disc samples (3.14 cm^2) were collected using a frost clamp whereafter the discs were placed in foil packets in liquid nitrogen and stored at -80°C. These additional leaf disc samples were collected in order to determine the influence of SO_2 on Rubisco.

3.4.4.2. Enzyme extraction assay

For the enzyme extraction, leaf material was weighed and ground finely with a pre-cooled mortar and pestle. Fifty mg acid washed sand and 20 mg PVPP was added into the mortar before grinding. One gram of leaf material was homogenised in 7 ml (80 mM) Potassium phosphate extraction buffer (pH = 7). Just before usage 0.0093 g EDTA (0.2 mM) and 0.0038 g DTT (2mM) were added per 25 ml buffer. The mixture was then centrifuged at 18 000 rpm for 30 minutes at 4 °C. The supernatant was used as the crude enzyme extract.

3.4.4.3. Peroxidase assay

POD activity was detemined by adding the following into a 1.5 ml quartz cuvette: 500 µl of a potassium phosphate buffer (pH = 7); 100 µl 0.018 M guaiacol; 50 µl of a 8.2 mM H_2O_2 substrate;

340 µl distilled H_20 and finally 10 µl enzyme extract. The change in absorbance of the contents is then measured spectophotometrically at 470 nm for 180 s (Zieslin & Ben-Zaken, 1991).

3.4.4.4. Protein concentration assay

The protein concentration of the extract was determined according to the method of Bradford (1976) using BSA as a standard. This method involves the binding of Coomassie Brilliant Blue G-250 to protein (BSA) where the increase in absorption at 595 nm is monitored. By using a Berthold LB 941 Multimode microplate reader, the absorbance was measured for a time period of 180 seconds. The assay mixture consisted of 150 µl ultra pure water, 40 µl BioRAD and 10 µl extract and for the protein standard 10 µl of a 0.5 µg/µl globulin solution was used.The contents were mixed automatically in the Microplate Reader and the absorbance at 595 nm was measured against a reagent blank prepared by adding 40 µl BioRAD to 160 µl ultra pure water. The protein standard curve was used to determine the unknown protein concentration of the samples.

3.4.4.5. Hydrogen peroxide content

Hydrogen peroxide content was determined by slightly modifying the method described by Brennan & Frenkel (1975). Hydroperoxides form a specific complex whith titanium (Ti^{4+}) which can be measured by colometry (Macnevin & Urone, 1953). After 1 g plant material was homogenised in 2 ml ice cold acetone, the extract was centrifuged for 20 minutes at 1250xg. 0.5 ml of a titanium reagent (20 % titanic tetrachloride in concentrated HCl, v/v) was added to the supernatant. Whilst shaking the solution, 3.5 ml NH_4OH (1/5 strength) was added drop wise to the peroxide-titanium complex. After centrifuging the solution for 5 minutes at 5000xg, the precipitate was washed repeatedly with 5 ml acetone until the supernatant was rendered collourless. The supernatant was discarded and the precipitate solubilised in 2 N H_2SO_4, and the final volume made up to 20 ml with H_2SO_4. Samples were left to stand a few minutes and the absorbance of the clear solution was read at 415 nm. Standards in the range of 0.1 to 0.5 mmol H_2O_2 ml^{-1} were also reacted with $TiCl_4$ and carried through the procedure.

3.5. Statistical analysis

Statistical analysis was implemented using the Statistica software package for Windows version 6 (StatSoft, Inc., USA). In data sets with parametric distribution, significant differences between treatment means were determined using the Student's t-test.